B$_{12}$-dependent photoresponsive protein hydrogels for controlled stem cell/protein release

Ri Wang[a,b,1], Zhongguang Yang[a,1], Jiren Luo[a], I-Ming Hsing[a,b], and Fei Sun[a,b,c,2]

[a]Department of Chemical and Biomolecular Engineering, The Hong Kong University of Science and Technology, Clear Water Bay, Kowloon, Hong Kong; [b]Division of BioMedical Engineering, The Hong Kong University of Science and Technology, Clear Water Bay, Kowloon, Hong Kong; and [c]Center for Systems Biology & Human Health, The Hong Kong University of Science and Technology, Clear Water Bay, Kowloon, Hong Kong

Thanks to the precise control over their structural and functional properties, genetically engineered protein-based hydrogels have emerged as a promising candidate for biomedical applications. Given the growing demand for creating stimuli-responsive "smart" hydrogels, here we show the synthesis of entirely protein-based photoresponsive hydrogels by covalently polymerizing the adenosylcobalamin (AdoB$_{12}$)-dependent photoreceptor C-terminal adenosylcobalamin binding domain (CarH$_C$) proteins using genetically encoded SpyTag-SpyCatcher chemistry under mild physiological conditions. The resulting hydrogel composed of physically self-assembled CarH$_C$ polymers exhibited a rapid gel-sol transition on light exposure, which enabled the facile release/recovery of 3T3 fibroblasts and human mesenchymal stem cells (hMSCs) from 3D cultures while maintaining their viability. A covalently cross-linked CarH$_C$ hydrogel was also designed to encapsulate and release bulky globular proteins, such as mCherry, in a light-dependent manner. The direct assembly of stimuli-responsive proteins into hydrogels represents a versatile strategy for designing dynamically tunable materials.

hydrogels | cell encapsulation | drug delivery | photoresponsive materials | protein engineering

Hydrogels, noted for their biomimetic properties, are the leading materials for biomedical applications, such as drug delivery and stem cell therapy (1, 2). Traditional hydrogels made up of either synthetic polymers or natural biomolecules often serve as passive scaffolds for molecular or cellular species, which render these materials unable to fully recapitulate the dynamic signaling involved in biological processes, such as cell/tissue development. It is, therefore, increasingly important to design stimuli-responsive, dynamic hydrogels that can accommodate or mimic the complexity of biological systems (3, 4). Photoresponsive hydrogels are of particular interest to material scientists, because light is regarded as an ideal tool to control molecules or cell behavior with high spatiotemporal precision and little invasiveness (5–9). Thanks to the advancement of synthetic chemistry, tremendous progress has been made over the past few years in making photoresponsive hydrogels with dynamically tunable properties (10, 11). Through a combination of orthogonal click reactions and photochemistry, some of these synthetic hydrogels can be mechanically and chemically patterned in situ by light while being used for 3D cell culturing (12, 13). Diverse photoactive chemical moieties have also been incorporated into synthetic hydrogels to create photoresponsive devices for controlled therapeutic release (5, 14, 15).

Assembling genetically engineered proteins into molecular networks represents an alternative strategy to make hydrogels with well-controlled properties (16–19). Although natural evolution has led to numerous functional protein domains that can sense and respond to a variety of environmental stimuli, such as light, oxidative stress, pH, small molecules, metal ions, etc., such ecological diversity has yet to be fully tapped to develop responsive biomaterials with dynamically tunable properties. The early work led by Murphy and coworkers (20, 21) showed the success of synthesizing calmodulin-based protein hydrogels with dynamic properties

responsive to Ca^{2+} and the small-molecule ligand trifluoperazine. Recently, the CarH protein, a transcriptional regulator controlling bacterial carotenoid synthesis, has been shown to sense and respond to visible light through its C-terminal adenosylcobalamin binding domain (CarH$_C$) (22–25). The CarH$_C$ domains tetramerize when binding to adenosylcobalamin (AdoB$_{12}$) in the dark and can readily dissociate into monomers accompanied with a drastic protein conformational change caused by the cleavage of the C-Co bond on exposure to green (522 nm) or white light (Fig. 1A) (23, 24). We envisioned that the light-sensing CarH$_C$ domains could be used to construct protein-based photoresponsive hydrogels. To this end, the major challenge is in how to assemble these complex globular proteins into supramolecular architectures efficiently while preserving their function.

Genetically encoded SpyTag (A)-SpyCatcher (B) chemistry, inspired by an isopeptide bond-containing bacterial adhesin, consists of a peptide/protein pair that can spontaneously form an isopeptide bond on binding under mild physiological conditions (26). Because of its high efficiency and modularity, this chemistry has led to a number of applications, including control of biomacromolecular topology, synthesis of bioactive and "living" materials, and biomolecular imaging (16, 18, 27–36). It has proven to be a powerful method for constructing complex biomolecular architectures both in vitro and in vivo. In this study, we successfully polymerized the elastin-like polypeptide (ELP)-fusion CarH$_C$ protein using SpyTag-SpyCatcher chemistry. CarH$_C$ tetramerization in the presence of AdoB$_{12}$ in the dark eventually led to the formation of a hydrogel that can undergo

Significance

Photoresponsive hydrogels have lately received ample attention because of their great potential in biomedical applications. However, the use of an entirely recombinant protein-based hydrogel with light-sensing abilities for stem cell applications has rarely been shown. Here, we created a B$_{12}$-dependent light-sensing hydrogel by covalently stitching together the photoreceptor C-terminal adenosylcobalamin binding domain (CarH$_C$) proteins under mild conditions. The polymeric CarH$_C$ proteins self-assemble into an elastic hydrogel in the presence of adenosylcobalamin in the dark and disassemble rapidly on light exposure. Such a photoresponsive protein hydrogel system enabled facile release/recovery of stem cells and protein molecules. This direct assembly of stimuli-responsive proteins into hydrogels represents a versatile strategy for designing "smart" materials and opens up enormous opportunities for future material biology.

Fig. 1. Synthesis of photoresponsive CarH$_C$ hydrogels. (A) Light exposure disassembles tetrameric CarH$_C$ accompanied by the degradation of AdoB$_{12}$, the release of 4′,5′-anhydroadenosine, and the coordination of His132 to the metal center. Tetrameric CarH$_C$ (Protein Data Bank ID code 5C8A). Monomeric CarH$_C$ (Protein Data Bank ID code 5C8F). (B) The two telechelic proteins, ACA and BCB, are polymerized through SpyTag-SpyCatcher chemistry. The resulting polymers can further be assembled into a molecular network through AdoB$_{12}$-induced CarH$_C$ tetramerization in the dark and disassembled on light exposure. ApoCarH$_C$ is the CarH$_C$ protein without AdoB$_{12}$. hv, light.

a rapid gel-sol transition on light exposure. This result illustrates a versatile strategy for developing stimuli-responsive protein materials for biomedical applications, such as controlled therapeutic release and cell recovery, from 3D cultures.

Results and Discussion

Protein Construct Design. To polymerize CarH$_C$, we designed two gene constructs encoding the telechelic proteins SpyTag-elastin-like polypeptide-C-terminal adenosylcobalamin binding domain-elastin-like polypeptide-SpyTag (ACA; 41 kDa) and SpyCatcher-elastin-like polypeptide-C-terminal adenosylcobalamin binding domain-elastin-like polypeptide-SpyCatcher (BCB; 68 kDa), respectively (Fig. 1B). The ELP domain consists of repeating pentapeptides (VPGXG)$_{15}$,

where X represents either valine or glutamate at a ratio of 4:1, a composition that is expected to enhance the expression yield and solubility of these recombinant proteins under physiological conditions (37). We envisioned that the reaction of SpyTag and SpyCatcher should be able to covalently stitch together CarH$_C$ to form protein polymers, of which interchain interactions will be dominated by the AdoB$_{12}$-induced CarH$_C$ tetramerization (Fig. 1B).

Synthesis of CarH$_C$ Hydrogels. Using an *Escherichia coli* expression system, we were able to produce and isolate sufficient amounts of the ACA (∼98 mg/L) and BCB (∼66 mg/L) proteins with high purity (*SI Appendix,* Figs. S1–S3). After extensive dialysis against distilled water and lyophilization, the resulting protein powders can

Wang et al.

www.manaraa.com

be readily dissolved in PBS. The two protein solutions, ACA and BCB (10 wt % in PBS), were mixed at an equimolar ratio immediately followed by addition of a stoichiometric amount of $AdoB_{12}$ to initiate gelation at room temperature in the dark. A red gel-like material was formed within 5 min; the gelation typically continued for at least 7 h in the dark before any subsequent analysis. The resulting gel was sensitive to light and converted to liquid on exposure to white LED light (30 klux) within 20 min (Fig. 2B). The observed gel-sol transition can be explained by the light-induced disassembly of $CarH_C$ tetramers (Fig. 1). A subsequent size-exclusion chromatography (SEC) analysis showed that the major elution peak of the light-degraded products as well as that of the reaction products of ACA + BCB in the absence of $AdoB_{12}$ appeared at the void volume (V_0; 8.7 mL), corresponding to a molecular weight that exceeds the exclusion limit ($\sim 2 \times 10^6$) (*SI Appendix*, Fig. S4). This SEC result further confirmed a sufficient polymerization of the $CarH_C$ proteins enabled by the SpyTag-SpyCatcher reaction during gelation.

Physical Properties of $CarH_C$ Hydrogels. Dynamic shear rheology was performed to monitor the gelation process. Simply mixing ACA and BCB in the absence of the $AdoB_{12}$ cofactor only led to a liquid-like material that exhibited a very low storage modulus G′ (Fig. 2A). However, the reaction of ACA + BCB in the presence of $AdoB_{12}$ under dark conditions led to a gradually increased storage modulus G′ that reached a steady value of ~0.66 kPa after 7 h and a much lower loss modulus G″ (~0.04 kPa), suggesting that $AdoB_{12}$-mediated $CarH_C$ tetramerization is essential for the hydrogel formation (Fig. 2A). The G′ of the hydrogel quickly dropped under constant light exposure, reflecting a typical gel-sol transition process (Fig. 2B), and the rates of the transition are affected by the light intensity (Fig. 2C). A stepwise gel-sol transition was also achieved by exposing the hydrogel to a pulsed light (Fig. 2D). Given the noncovalent nature of $CarH_C$ tetramerization, we speculated that the $CarH_C$ hydrogel composed of ACA + BCB would display frequency-dependent viscoelastic properties. However, the frequency sweep test on the $CarH_C$ hydrogel at room temperature (25 °C) showed a steady storage modulus

(0.58–0.81 kPa) over an angular frequency of 0.01–100 rad/s (*SI Appendix*, Fig. S5A), which is indicative of static interchain interactions. One possible explanation is that the $CarH_C$ tetramers within the hydrogel network are kinetically inert, of which the disassembly or exchange takes longer than the timescale for the lowest shear frequency tested (628 s). Assuming that all of the $CarH_C$ domains form tetramers, a theoretical estimate of the G′ of the $CarH_C$ hydrogel (8.3 wt %) is ~0.94 kPa based on G = ρRT/M_c, where the average molecular mass between cross-links M_c is ~218 kDa (2ACA + 2BCB). The observed G′ matches well with the theoretical estimate, suggesting the sufficient assembly of the $CarH_C$ domains within the hydrogel network. The $CarH_C$ hydrogel also exhibited stability toward mechanical deformation (1–10% strain) as revealed by the strain-sweep test at room temperature (*SI Appendix*, Fig. S5B).

The ELP domains are known to have a unique phase transition behavior at a so-called lower critical solution temperature (LCST). The LCST of the ELP domain that we chose is 25 °C to 30 °C (37). To investigate the influence of temperature on these ELP-based hydrogel properties, we performed rheology studies on the hydrogels at different temperatures (16 °C, 25 °C, and 37 °C) and observed little change in their rheological behaviors, suggesting that the phase transition of ELPs has negligible effects on macroscopic mechanical properties of the materials.

The $CarH_C$ hydrogel composed of ACA + BCB + $AdoB_{12}$ exhibited moderate swelling in PBS at room temperature, and the swelling ratio, calculated as the ratio of the wet gel weight to the dry protein weight, reached maximum (~25) from an initial ratio of 12 within 3 d (*SI Appendix*, Fig. S6). The hydrogel is also stable. Only ~6% of the gel was eroded in the presence of excess PBS at room temperature after 10 d (*SI Appendix*, Fig. S7).

Cell Encapsulation and Light-Induced Release/Recovery. For the study of cell matrix interactions as well as tissue engineering, it is desirable to have a 3D cell culture system that allows cells to be encapsulated and readily released/recovered without resorting to complicated chemical or proteolytic degradation (38, 39). The $CarH_C$ hydrogel composed of ACA + BCB + $AdoB_{12}$ that undergoes a rapid gel-sol transition on light exposure may allow us to handily recover/release cells after 3D culturing. We first examined the cytocompatibility of the $CarH_C$ hydrogel using mouse 3T3 fibroblasts and human mesenchymal stem cells (hMSCs). To encapsulate the cells, the BCB solution containing the cells was mixed thoroughly with the ACA solution at a 1:1 molar ratio followed by adding a stoichiometric amount of $AdoB_{12}$ to initiate gelation in the dark. After 2 h of curing, the gels were covered with culture medium and incubated under standard conditions (37 °C at 5% CO_2) away from light. After 24 h, a live/dead staining was performed to examine the cell viability. It turned out that most of the embedded fibroblasts (88 ± 3%) and mesenchymal stem cells (MSCs; 92 ± 2%) remained viable (Fig. 3), suggesting that the $CarH_C$ hydrogel is nontoxic to these cells.

Rapid gelation is required by cell encapsulation applications. The gelation rate of the current $CarH_C$ hydrogel system mainly depends on two events: the SpyTag-SpyCatcher reaction and $AdoB_{12}$-dependent $CarH_C$ self-assembly. The SpyTag-SpyCatcher reaction is likely to be the rate-limiting step, because its second-order rate constant is ~1.4 × 10^3 M^{-1} s^{-1}, which is far from the diffusion limit and substantially slower than some other biomolecular interactions, such as the widely used streptavidin–biotin interaction (26). The reaction kinetics of SpyTag-SpyCatcher can be optimized through directed evolution to accelerate the gelation. Alternatively, the efficiency of $CarH_C$ self-assembly can also be improved through protein engineering, so that a hydrogel system solely based on the $CarH_C$ tetramerization can be developed to enable swift cell encapsulation.

To recover these encapsulated cells, we exposed the cell-laden gels to white light. The cells gradually migrated along with the
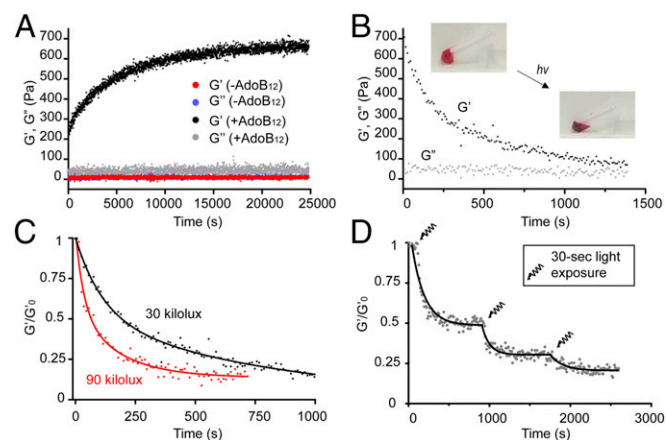
Fig. 2. $AdoB_{12}$-dependent photoresponsiveness of $CarH_C$ hydrogels. (*A*) Evolution of the storage modulus G′ and loss modulus G″ of ACA + BCB in the presence and absence of $AdoB_{12}$ at room temperature (25 °C) in the dark as a function of time. (*B*) Gel-sol transition induced by light. On white LED light exposure (30 klux), the G′ and G″ of the $CarH_C$ hydrogel were monitored at a fixed shear frequency of 1 rad/s and strain of 5%. (*C*) Gel-sol transition rates of the $CarH_C$ hydrogels are affected by light intensity. The normalized storage modulus (G′/G′$_0$) of the materials exposed to the 30- and 90-klux lights is compared. The G′ values corresponding to the 30-klux light exposure were from the same measurement shown in *B*. (*D*) Response of the $CarH_C$ hydrogel toward pulsed light (90 klux). Exponential decay curve fitting was used. hv, light.
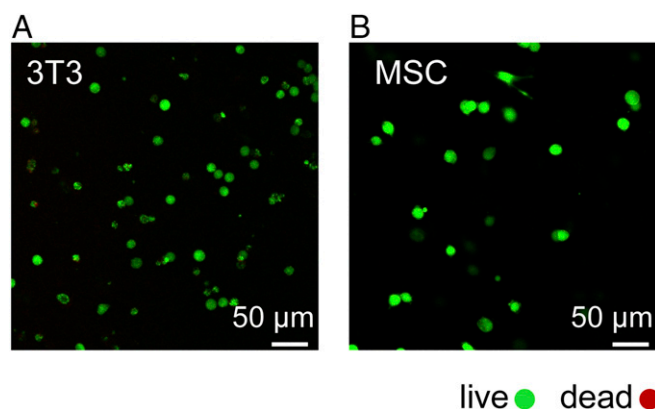
Fig. 3. Encapsulation of (*A*) 3T3 fibroblasts and (*B*) MSCs by the physically assembled CarH$_C$ hydrogels composed of ACA + BCB + AdoB$_{12}$. Representative confocal fluorescence *z*-slice micrographs of live (green; calcein AM) and dead (red; ethidium homodimer) cells are shown.

melting gel, suggesting that these cells were indeed encapsulated in a 3D manner (Fig. 4 and Movies S1 and S2). Within 5 min, the gels were completely transformed into liquid accompanied with a complete release of the cells. The live/dead staining showed that the majority of recovered cells (3T3: 90 ± 7%; MSCs: 88 ± 5%) remained viable, indicating that the photolysis of the CarH$_C$ hydrogels is amicable to the encapsulated cells (Fig. 4 *B* and *D*). The photodegradation of AdoB$_{12}$ in CarH does not use a typical radical mechanism, and its photolytic product is 4′,5′-anhydroadenosine instead of more common 5′-dAdo radicals (25, 40). Although adenosine could lead to cytotoxicity at relatively high concentrations or after prolonged exposure, so far, there has been no direct evidence pointing to the cytotoxicity or any other side effect of its analog 4′,5′-anhydroadenosine on cell phenotypes (41). In addition, only trace amounts of unbound AdoB$_{12}$ (∼1 μM) exists in the CarH$_C$ hydrogel (8.3 wt %) given the dissociation constant K_d for the AdoB$_{12}$–CarH complex (0.8 μM) (24). Therefore, the radical species resulting from the photolysis of the free AdoB$_{12}$ is negligible and can hardly cause cytotoxicity. Both the nonradical photolysis of the AdoB$_{12}$ binding CarH$_C$ and the very low concentration of the free AdoB$_{12}$ likely contribute to the high viability of these cells recovered from the protein hydrogels.

Light-Induced Protein Release.

Protein drugs, an important category of modern therapeutics, have a short half-life time inside the body because of rapid plasma clearance and proteolytic degradation, which constitutes a fundamental challenge for their delivery (42, 43). The ELP fusion strategy has previously been shown to be able to significantly enhance pharmacokinetics and efficacy of a protein drug by prolonging its circulating half-life (44). It prompted us to examine the feasibility of using the photoresponsive CarH$_C$-ELP hydrogel system to encapsulate and release protein molecules in a controlled manner. Inspired by the previously reported Spy network hydrogel (16), we chose two recombinant proteins, SpyTag-elastin-like polypeptide-SpyTag-elastin-like polypeptide-SpyTag (AAA) (*SI Appendix*, Figs. S1 and S8) and BCB, to synthesize a covalently cross-linked ELP hydrogel. The two proteins were dissolved in PBS to make 10 wt % solutions. Gelation was initiated by mixing the two components at a 2:3 molar ratio and a stoichiometric amount of AdoB$_{12}$ in the dark. Dynamic shear rheology experiments in time-, frequency- and strain-sweep modes and erosion tests further confirmed the formation of a stable hydrogel (G′ = 0.96 kPa and G″ = 0.03 Pa) by AAA + BCB + AdoB$_{12}$ (*SI Appendix*, Figs. S9 and S10).

To test the feasibility of this covalently cross-linked CarH$_C$ hydrogel for controlled protein release, a recombinant CarH$_C$-fusion mCherry protein was constructed and used as a model substrate (*SI Appendix*, Figs. S1 and S11). We envisioned that the mCherry-CarH$_C$ protein could be physically tethered to the hydrogel network through AdoB$_{12}$-dependent CarH$_C$ self-assembly in the dark and that light exposure would disassemble the CarH$_C$ tetramers and facilitate the release of mCherry-CarH$_C$ (Fig. 5*A*). To test this hypothesis, three sets of mCherry-CarH$_C$–decorated hydrogels were synthesized and immersed in PBS; two were exposed to the white LED light (90 klux) for 1 and 10 min before being moved to the dark, and the third one was kept in the dark all of the time. Aliquots of the supernatant were taken to analyze the release of mCherry over 24 h. Fig. 5*B* shows that about 24 and 45% of mCherry-CarH$_C$ were released from the gels that were subjected to 1- and 10-min light exposure, respectively, after 24 h, whereas the release was substantially slower in the gel always kept in the dark with less than 10% of mCherry-CarH$_C$ released. This result suggests that controlled protein release in this system can be readily achieved by adjusting the duration of the light exposure. For the mCherry protein lacking the CarH$_C$ domain, its release from the AAA + BCB hydrogel was light-independent, because similar amounts of free mCherry (∼50%) were detected in the supernatants under the dark and bright conditions, further corroborating that the CarH$_C$ domain
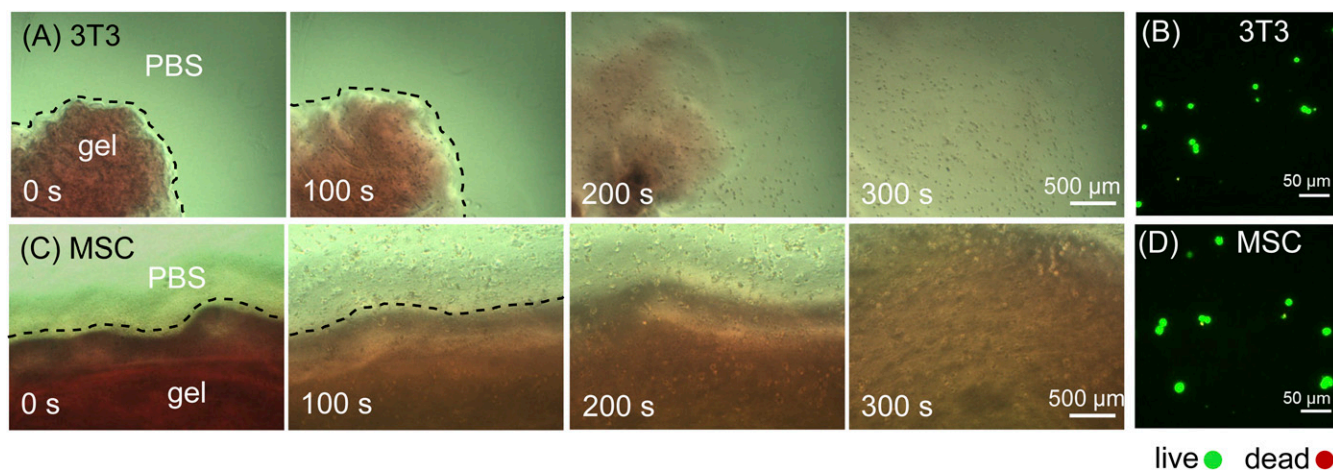
Fig. 4. Release of encapsulated cells by light-induced gel-sol transition. (*A*) Mouse 3T3 fibroblasts and (*C*) hMSCs were encapsulated by CarH$_C$ hydrogels (red) and cultured for 24 h. Cell release was initiated by exposing the 3D cell culture to white light (22 klux). Representative bright-field micrographs (0, 100, 200, and 300 s after light exposure) are shown. Dashed lines indicate the gel boundaries. (*B* and *D*) Live/dead staining of recovered 3T3 fibroblasts and hMSCs.

Wang et al.
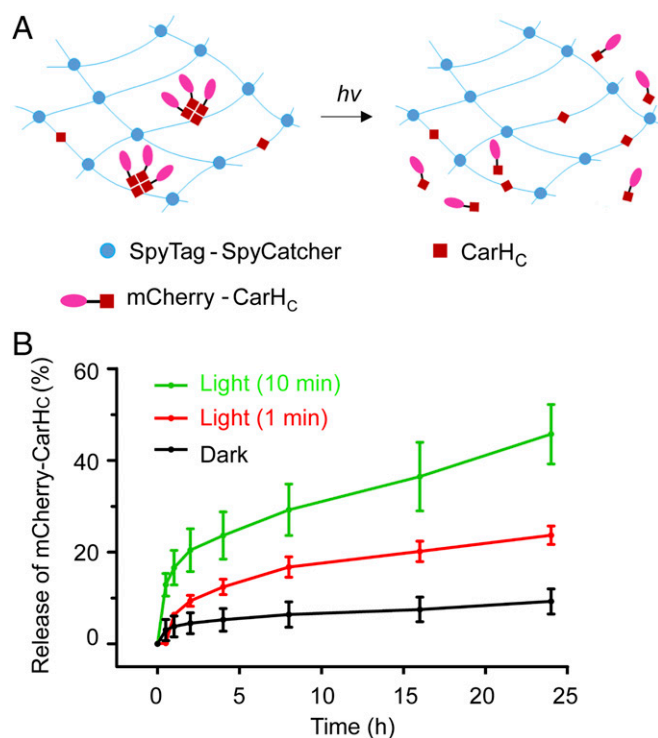
Fig. 5. Protein immobilization and light-induced release enabled by the covalently cross-linked $CarH_C$ hydrogels. (*A*) Schematic showing the immobilization and release of the mCherry-$CarH_C$ protein. The hydrogel (8.6 wt %) is composed of AAA and BCB at a 2:3 molar ratio, a stoichiometric amount of $AdoB_{12}$, and the fusion protein mCherry-$CarH_C$ (50 µM). $CarH_C$ tetramerization leads to the mCherry immobilization into the hydrogel in the dark. The photolysis of $AdoB_{12}$ disassembles tetrameric $CarH_C$ and facilitates the release of mCherry-$CarH_C$. (*B*) Release profiles of mCherry-$CarH_C$ from the hydrogels that were subjected to 0, 1, and 10 min of white light exposure. The percentage release of mCherry was calculated based on the total amount of mCherry added into the gel. Error bars show SDs from three independent measurements. hv, light.

is essential for the light-controlled release (*SI Appendix*, Fig. S12). It is also noteworthy that, despite two tobacco etch virus (TEV) protease cleavage sites in the BCB construct, the covalently cross-linked hydrogels composed of AAA + BCB + $AdoB_{12}$ are resistant toward TEV digestion at room temperature under both dark and bright (white LED light; 90 klux) conditions (*SI Appendix*, Fig. S13). These ELP-based covalent networks likely served as physical barriers to protect the encapsulated proteins/peptides from proteolysis, even after photolysis. These results together show the feasibility of using the photoresponsive $CarH_C$ hydrogel for controlled protein delivery/release.

In summary, we have reported the creation of entirely recombinant protein-based light-sensitive hydrogels by covalently assembling the $CarH_C$ photoreceptor proteins using SpyTag-SpyCatcher chemistry. The $AdoB_{12}$-dependent $CarH_C$ tetramerization has been shown to be essential for the formation of an elastic hydrogel in the dark, which can undergo a rapid gel-sol transition caused by light-induced $CarH_C$ disassembly. Such photoresponsiveness has been used for facile release/recovery of fibroblasts and MSCs from 3D cultures as well as controlled release of protein molecules. This $CarH_C$ hydrogel system represents an example of using $AdoB_{12}$ photochemistry to control the material properties and thus, points to a versatile strategy for creating photoresponsive materials.

Experimental Procedures

Gene Construction and Protein Expression. Plasmids, such as pQE80l::*SpyTag-ELP-RGD-ELP-SpyTag* (*AA*), pQE80l::*SpyTag-ELP-SpyTag-ELP-SpyTag* (*AAA*), and pQE80l::*SpyCatcher-ELP-SpyCatcher* (*BB*), were constructed as described

previously (7). The *carH_C* gene was purchased as a gBlocks gene fragment from Integrated DNA Technologies. pQE80l::*SpyTag-ELP-carH_C-ELP-SpyTag* (*ACA*) and pQE80l::*SpyCatcher-ELP-carH_C–ELP-SpyCatcher* (*BCB*) were constructed by replacing the middle *RGD* site with *carH_C* in pQE80l::*AA* and pQE80l::*BB*, respectively. SacI and SpeI restriction sites were used. pET22b::*mCherry-carH_C* was constructed by inserting the *mCherry* gene into a pET22b-derived plasmid carrying a *carH_C* gene, and NdeI and SacI restriction sites were used. *E. coli* strain DH5α was used for plasmid amplification.

E. coli strain BL21 (DE3) was the bacterial host for protein expression. The bacterial cells were grown at 37 °C in LB to the midlog phase (OD at 600 nm, ~0.6–0.8) followed by adding 1 mM isopropyl β-D-1-thiogalactopyranoside (Sangon Biotech) to induce protein expression at 37 °C. After 4 h, cells were harvested and flash-frozen in liquid N_2 before protein purification. The proteins were purified on HisTrap columns (GE Healthcare, Inc.) following the column manufacturer's recommendations. The purified proteins were dialyzed against Milli-Q water (5 L × 4) at 4 °C and lyophilized at −100 °C. Lyophilized proteins were stored at −80 °C before use.

Hydrogel Preparation. The ACA and BCB proteins were dissolved in PBS to yield 10 wt % solutions. $AdoB_{12}$ (Shaanxi Pioneer Biotech) was dissolved in PBS to a final concentration of 9.2 mM. ACA and BCB were mixed at an equimolar ratio followed by addition of a stoichiometric amount of $AdoB_{12}$ in the dark at room temperature.

Dynamic Shear Rheology. Dynamic time-, strain-, and frequency-sweep experiments were performed on a TA Instruments ARES-RFS strain-controlled rheometer with a standard steel parallel-plate geometry (8-mm diameter). Gelation of the mixture of 31 µL BCB (10 wt % in PBS), 19 µL ACA (10 wt % in PBS), and 10 µL $AdoB_{12}$ (9.2 mM in PBS) was monitored by time-sweep measurement, with strain and frequency fixed at 5% and 1 rad/s, respectively, at 25 °C for 7 h. Strain sweep was performed from 0.1 to 10% at a fixed frequency of 1 rad/s at 25 °C. Frequency sweep was performed from 100 to 0.01 rad/s by holding the strain at 5% at the temperature indicated (16, 25, or 37 °C). All of the samples were wrapped with aluminum foil to avoid light during the rheological measurements. Photolysis was conducted by exposing the $CarH_C$ hydrogel to white LED light (30 or 90 klux), and dynamic time sweep was used to monitor the gel-sol transition.

Protein Immobilization and Light-Induced Release. The AAA and BCB proteins and the $AdoB_{12}$ cofactor were dissolved in the PBS solution containing mCherry-$CarH_C$ or mCherry (50 µM) to yield 10 wt % protein solutions for AAA and BCB and a 9.2 mM solution for $AdoB_{12}$, respectively. Hydrogels were prepared by mixing the three solutions 36 µL BCB, 7.5 µL AAA, and 7 µL $AdoB_{12}$ and cured in the dark for 24 h. To examine the effect of light on the protein release, the gels were either exposed to white LED light (90 klux) for 10 min or constantly kept in the dark as a control. Both groups of samples were immersed with 500 µL PBS and transferred to the dark. To determine the amounts of protein released into the supernatant, aliquots (100 µL) were taken for fluorescence measurements (excitation at 587 nm and emission at 610 nm) with a Varioskan LUX multimode microplate reader (Thermo Scientific) at different time points, and 100 µL fresh PBS was added back to keep the supernatant volume constant.

Encapsulation and Light-Induced Release of 3T3 Fibroblasts and hMSCs. NIH/3T3 mouse embryonic fibroblasts were cultured in high-glucose DMEM (Sangon Biotech) supplemented with 10% (vol/vol) FBS (Sangon Biotech), 1% (vol/vol) penicillin-streptomycin (Sangon Biotech), and 1% (vol/vol) nonessential amino acids (Sangon Biotech) in a 5% CO_2 atmosphere at 37 °C and passaged every 3 d. At 70–80% confluence, cells were detached with 1 mL trypsin solution (Sangon Biotech) followed by addition of 2 mL DMEM to neutralize the trypsin. Around 60,000 cells were pelleted and resuspended with 31 µL BCB in DMEM (10 wt %) and then placed on a cell culture dish with a coverslip bottom. Gelation was initiated by adding 19 µL ACA in PBS (10 wt %) and 10 µL $AdoB_{12}$ in PBS (9.2 mM). The gel was cured in the dark for 2 h before being covered with the culture medium. After 24 h of incubation and washing with Dulbecco's PBS (Sangon Biotech), live/dead cell viability assays (Thermo Fisher Scientific) were conducted. Fluorescence images were obtained on a Laser Scanning Confocal Microscope [LSM7 DUO (710 + LIVE); Zeiss].

hMSCs were provided as a gift from Chao Wan, Chinese University of Hong Kong, Hong Kong. The cells were cultured at 37 °C with 5% CO_2 in MEM Alpha (Gibco) supplemented with 10% (vol/vol) FBS (Gibco), 2 mM L-glutamine, and 1% (vol/vol) penicillin-streptomycin. Cells were passaged every 5–6 d using 0.25% trypsin (Sangon Biotech) solution. The encapsulation procedure was similar to that of 3T3 fibroblasts as described above.

For cell release/recovery experiments, cell-laden gels were rinsed and immersed by PBS before exposure to white light (halogen lamp in the microscope, ~22 klux). Cell release was monitored and recorded with an optical microscope

www.manaraa.com

equipped with a camera (Olympus CKX41). The live/dead staining assay was performed to examine the viability of recovered cells. Quantification of cell viability was done by counting live and dead cells in the micrographs ($n \geq 4$) that were randomly chosen.

1. Lee KY, Mooney DJ (2001) Hydrogels for tissue engineering. *Chem Rev* 101: 1869–1879.
2. DeForest CA, Anseth KS (2012) Advances in bioactive hydrogels to probe and direct cell fate. *Annu Rev Chem Biomol Eng* 3:421–444.
3. Langer R, Tirrell DA (2004) Designing materials for biology and medicine. *Nature* 428: 487–492.
4. Burdick JA, Murphy WL (2012) Moving from static to dynamic complexity in hydrogel design. *Nat Commun* 3:1269.
5. DeForest CA, Anseth KS (2011) Cytocompatible click-based hydrogels with dynamically tunable properties through orthogonal photoconjugation and photocleavage reactions. *Nat Chem* 3:925–931.
6. Tomatsu I, Peng K, Kros A (2011) Photoresponsive hydrogels for biomedical applications. *Adv Drug Deliv Rev* 63:1257–1266.
7. Katz JS, Burdick JA (2010) Light-responsive biomaterials: Development and applications. *Macromol Biosci* 10:339–348.
8. Yagai S, Kitamura A (2008) Recent advances in photoresponsive supramolecular self-assemblies. *Chem Soc Rev* 37:1520–1529.
9. Deisseroth K (2011) Optogenetics. *Nat Methods* 8:26–29.
10. Ercole F, Davis TP, Evans RA (2010) Photo-responsive systems and biomaterials: Photochromic polymers, light-triggered self-assembly, surface modification, fluorescence modulation and beyond. *Polym Chem* 1:37–54.
11. Fairbanks BD, Scott TF, Kloxin CJ, Anseth KS, Bowman CN (2009) Thiol-Yne photopolymerizations: Novel mechanism, kinetics, and step-growth formation of highly cross-linked networks. *Macromolecules* 42:211–217.
12. DeForest CA, Polizzotti BD, Anseth KS (2009) Sequential click reactions for synthesizing and patterning three-dimensional cell microenvironments. *Nat Mater* 8:659–664.
13. DeForest CA, Tirrell DA (2015) A photoreversible protein-patterning approach for guiding stem cell fate in three-dimensional gels. *Nat Mater* 14:523–531.
14. Alvarez-Lorenzo C, Bromberg L, Concheiro A (2009) Light-sensitive intelligent drug delivery systems. *Photochem Photobiol* 85:848–860.
15. Fairbanks BD, et al. (2009) A versatile synthetic extracellular matrix mimic via thiol-norbornene photopolymerization. *Adv Mater* 21:5005–5010.
16. Sun F, Zhang WB, Mahdavi A, Arnold FH, Tirrell DA (2014) Synthesis of bioactive protein hydrogels by genetically encoded SpyTag-SpyCatcher chemistry. *Proc Natl Acad Sci USA* 111:11269–11274.
17. Banta S, Wheeldon IR, Blenner M (2010) Protein engineering in the development of functional hydrogels. *Annu Rev Biomed Eng* 12:167–186.
18. Gao X, Fang J, Xue B, Fu L, Li H (2016) Engineering protein hydrogels using SpyCatcher-SpyTag chemistry. *Biomacromolecules* 17:2812–2819.
19. Fang J, et al. (2013) Forced protein unfolding leads to highly elastic and tough protein hydrogels. *Nat Commun* 4:2974.
20. Murphy WL, Dillmore WS, Modica J, Mrksich M (2007) Dynamic hydrogels: Translating a protein conformational change into macroscopic motion. *Angew Chem Int Ed Engl* 46:3066–3069.
21. Sui ZJ, King WJ, Murphy WL (2008) Protein-based hydrogels with tunable dynamic responses. *Adv Funct Mater* 18:1824–1831.
22. Kutta RJ, et al. (2015) The photochemical mechanism of a B12-dependent photoreceptor protein. *Nat Commun* 6:7907.
23. Jost M, et al. (2015) Structural basis for gene regulation by a B12-dependent photoreceptor. *Nature* 526:536–541.
24. Ortiz-Guerrero JM, Polanco MC, Murillo FJ, Padmanabhan S, Elías-Arnanz M (2011) Light-dependent gene regulation by a coenzyme B12-based photoreceptor. *Proc Natl Acad Sci USA* 108:7565–7570.
25. Jost M, Simpson JH, Drennan CL (2015) The transcription factor CarH safeguards use of adenosylcobalamin as a light sensor by altering the photolysis products. *Biochemistry* 54: 3231–3234.
26. Zakeri B, et al. (2012) Peptide tag forming a rapid covalent bond to a protein, through engineering a bacterial adhesin. *Proc Natl Acad Sci USA* 109:E690–E697.
27. Schoene C, Fierer JO, Bennett SP, Howarth M (2014) SpyTag/SpyCatcher cyclization confers resilience to boiling on a mesophilic enzyme. *Angew Chem Int Ed Engl* 53:6101–6104.
28. Veggiani G, et al. (2016) Programmable polyproteams built using twin peptide superglues. *Proc Natl Acad Sci USA* 113:1202–1207.
29. Reddington SC, Howarth M (2015) Secrets of a covalent interaction for biomaterials and biotechnology: SpyTag and SpyCatcher. *Curr Opin Chem Biol* 29:94–99.
30. Chen AY, et al. (2014) Synthesis and patterning of tunable multiscale materials with engineered cells. *Nat Mater* 13:515–523.
31. Botyanszki Z, Tay PKR, Nguyen PQ, Nussbaumer MG, Joshi NS (2015) Engineered catalytic biofilms: Site-specific enzyme immobilization onto E. coli curli nanofibers. *Biotechnol Bioeng* 112:2016–2024.
32. Zhang WB, Sun F, Tirrell DA, Arnold FH (2013) Controlling macromolecular topology with genetically encoded SpyTag-SpyCatcher chemistry. *J Am Chem Soc* 135:13988–13997.
33. Matsunaga R, Yanaka S, Nagatoishi S, Tsumoto K (2013) Hyperthin nanochains composed of self-polymerizing protein shackles. *Nat Commun* 4:2211.
34. Fairhead M, et al. (2014) SpyAvidin hubs enable precise and ultrastable orthogonal nanoassembly. *J Am Chem Soc* 136:12355–12363.
35. Liu ZD, et al. (2014) A novel method for synthetic vaccine construction based on protein assembly. *Sci Rep UK* 4:7266.
36. Bedbrook CN, et al. (2015) Genetically encoded spy peptide fusion system to detect plasma membrane-localized proteins in vivo. *Chem Biol* 22:1108–1121.
37. Urry DW (1997) Physical chemistry of biological free energy transduction as demonstrated by elastic protein-based polymers. *J Phys Chem B* 101:11007–11028.
38. Santoro M, Tatara AM, Mikos AG (2014) Gelatin carriers for drug and cell delivery in tissue engineering. *J Control Release* 190:210–218.
39. Vo TN, Kasper FK, Mikos AG (2012) Strategies for controlled delivery of growth factors and cells for bone regeneration. *Adv Drug Deliv Rev* 64:1292–1309.
40. Sension RJ, Harris DA, Cole AG (2005) Time-resolved spectroscopic studies of B12 coenzymes: Comparison of the influence of solvent on the primary photolysis mechanism and geminate recombination of methyl-, ethyl-, n-propyl-, and 5'-deoxyadenosylcobalamin. *J Phys Chem B* 109:21954–21962.
41. Seetulsingh-Goorah SP (2006) Mechanisms of adenosine-induced cytotoxicity and their clinical and physiological implications. *Biofactors* 27:213–230.
42. Tessmar JK, Göpferich AM (2007) Matrices and scaffolds for protein delivery in tissue engineering. *Adv Drug Deliv Rev* 59:274–291.
43. Shah NJ, et al. (2014) Adaptive growth factor delivery from a polyelectrolyte coating promotes synergistic bone tissue repair and reconstruction. *Proc Natl Acad Sci USA* 111:12847–12852.
44. Hu J, Wang G, Liu X, Gao W (2015) Enhancing pharmacokinetics, tumor accumulation, and antitumor efficacy by elastin-like polypeptide fusion of interferon alpha. *Adv Mater* 27:7320–7324.

CHEMISTRY

BIOCHEMISTRY

www.manaraa.com